An Alternative Approach to Ascertain the Rate-Determining Steps of TiO₂ Photoelectrocatalytic Reaction by Electrochemical Impedance Spectroscopy

H. Liu,[†,‡] X. Z. Li,*[,†] Y. J. Leng,[§] and W. Z. Li[‡]

Department of Civil and Structural Engineering, The Hong Kong Polytechnic University,
Hunghom, Kowloon, Hong Kong, State Key Laboratory of Catalysis, Dalian Institute of Chemical Physics,
Chinese Academy of Sciences, Dalian 116023, China, and School of Mechanical and Production Engineering,
Nanyang Technological University, 50 Nanyang Avenue, Singapore 639798, Republic of Singapore

Received: January 16, 2003; In Final Form: June 15, 2003

In an attempt to ascertain the rate-determining steps (RDS) of TiO₂ photoelectrocatalytic (PEC) reaction, the PEC oxidation of sulfosalicylic acid (SSA) solution in a TiO₂-coated electrode reactor system was monitored by applying the electrochemical impedance spectroscopy (EIS) method. In the meantime, an EIS mathematical model was first established to theoretically simulate the PEC reaction. Based on the EIS model, the theoretical simulation indicates three typical reactions in a PEC oxidation process, which include the charge-transfer-dominated reaction, both the charge-transfer- and adsorption-dominated reaction, and the adsorption-dominated reaction. The experimental results of EIS measurement showed that there was only one arc/semicircle on the EIS plane display when the external bias applied was below 200 mV (vs SCE) in the SSA PEC degradation whereas there were two arcs/semicircles when the externally applied bias exceeded 200 mV (vs SCE). The experimental results have a good agreement with the model simulation. The EIS method in this study provides an easier way to determine the RDS in a PEC oxidation process, which would be helpful to better control the reaction in practice.

1. Introduction

Great attention has been paid to the photocatalytic reactions occurring on TiO₂ particles and much progress has been made in the last two decades.[1−3] It is commonly accepted that when the TiO₂ is photoexcited by light with energy greater than the TiO₂ band gap, holes and electrons are photogenerated. The photogenerated holes attack the −OH to produce •OH radicals, which can further oxidize the organic substrate adsorbed on the TiO₂ surface. At the same time, the photogenerated electrons can transfer to an oxidant. Thus it is believed that the key point to improve the activity of the TiO₂ is to enhance the separation rate of the e−h pairs and inhibit their recombination. Some researchers have already proved that an application of an external bias onto the TiO₂ electrode could enhance the charge separation.[4−10] This type of photoelectrocatalytic (PEC) method has been applied even in a pilot-scale water treatment as reported in 1999.[11]

In general, such a PEC process consists of the following steps: (1) mass transfer to approach the TiO₂ electrode surface, (2) adsorption of reactants onto the electrode surface, (3) chemical reaction on the surface, (4) desorption of the products from the electrode surface, and (5) mass transfer of the products from the electrode surface. Among these steps, there must be a step called the rate-determining step (RDS). It was found that the effect of mass transfer and desorption in a PEC system of biased TiO₂ films can be neglected because the photocurrent is not limited by the mass transfer and is insensitive toward stirring.[8] In fact, the mass transfer effect can commonly be precluded by stirring the reaction solution effectively.[4−10] On the other hand, some researchers stated that the adsorption is the prerequisite to the photocatalytic degradation,[12,13] and the adsorption of the organic substrate onto the TiO₂ electrode appears to be a vital factor. For example, Kesselman and co-workers found that the rate of 4-chlorocatechol degradation on illuminated TiO₂ electrode under a bias was affected strongly by the organic adsorption behavior.[7] Therefore, the major steps should be focused on the chemical reaction (charge transfer) and adsorption steps in the PEC process.

To investigate the RDS of a photocatalytic reaction, a set of kinetic experiments can be carefully designed and realistically conducted.[14,15] For example, through a series of kinetic experiments, Yamazaki et al. found that in the photocatalytic degradation of ethylene the RDS was the ethylene oxidation with oxygen on the TiO₂ surface.[14] However, we also realized that the kinetic method is a time-consuming procedure and has many limits due to the complexity of the PEC system. Especially, when other steps beyond the researchers' assumption were also included in the PEC reaction, it would be difficult to interpret the results by the common kinetic investigation. It is necessary to have some other convenient methods such as an in-situ one that can give more complete feedback information.

Electrochemical impedance spectroscopy (EIS)[16−18] appears to be able to meet this requirement for the following reasons. First, EIS is such a method that only a sinusoidal signal of small amplitude is superimposed onto the system, thus barely disturbing the characteristics of the steady state even with an applied voltage or illumination.[18] This method has an in situ characteristics. Second, the PEC reaction on the TiO₂ electrode surfaces, involving competition between interfacial charge separation and recombination of photogenerated e−h pairs, is itself a typical electrochemical reaction. Thus an electrochemical

* To whom correspondence should be addressed. Fax: (852)23346389. E-mail: cexzli@polyu.edu.hk.
† The Hong Kong Polytechnic University.
‡ Chinese Academy of Sciences.
§ Nanyang Technological University.

An Alternative Approach to Ascertain

J. Phys. Chem. B, Vol. 107, No. 34, 2003 **8989**

method is necessary to investigate it, and the EIS method is just such a method. Third, the EIS method is a frequency domain method, in which the response due to different processes can be recorded in a single frequency sweep. Even if there were some other steps in the electrode reaction beyond the investigators' assumption, such steps will be observed by the spectroscopy. Thus the EIS method can help to obtain more complete and richer information in this regard.

EIS is in fact a widely used electrochemical method, very effective to study the interface and its structure and the reactions taking place there. [16] Some researchers used this method to investigate the properties of the anodic oxidation film of TiO_2[17] or some porous TiO_2 electrodes[18] or the electron-transfer process across the semiconductor−molecular interfaces.[19] However, the study of PEC degradation reaction has not been widely conducted except few reports in our knowledge.[20,21] In our previous work,[20] the EIS method was employed to investigate the PEC reaction of sulfosalicylic acid (SSA). We have found only one arc on the EIS plane display that had a small size corresponding to a more rapid SSA degradation. The size of the EIS arc of the PEC degradation reflected the degradation rate of the organic substrate. However, we failed to explain this phenomenon. More recently, Leng et al. confirmed such results.[21] They found that the PEC degradation rate of aniline was inversely proportional to the value of charge-transfer resistance of photoelectrodes prepared by thermal oxidation on titanium.[21] To better interpret the EIS results, it is necessary to establish EIS mathematical models.

In this study, an EIS mathematical model for the PEC reaction was established and used to reveal the required PEC reaction. Then an EIS experiment of PEC oxidation was also conducted to confirm the indication from the theoretical simulation results.

2. Experimental Section

TiO_2 powder (30 nm, anatase) from Taixing, Jiangsu, China, was thermally treated by hydrogen gas (general grade) in a homemade quartz tube, which was placed in an oven and operated by a temperature controller.[22] The temperature increased from 20 °C to a designated level at an increasing rate of 10 °C min^{-1} and then was kept for 2 h. The gas flow rate was adjusted to be 30 mL min^{-1}. After that, the samples cooled to room temperature naturally. The TiO_2 sample treated with hydrogen was named H-TiO_2, while raw TiO_2 sample was called R-TiO_2.

The electrodes used in the EIS experiment were prepared by the following procedure. The TiO_2 powder (H-TiO_2 or R-TiO_2) was coated on a SnO_2 conducting glass substrate (resistance ca. 12 Ω/plate) using 3 wt % poly(vinyl alcohol) (PVA) as the binder. The SnO_2 glass was cleaned with absolute alcohol and distilled water before use. About 5 mg of TiO_2 powder was coated on each SnO_2 glass plate with an area of 1×1 cm^2. Prior to use in the EIS experiment, the TiO_2/SnO_2 electrode was kept in an oven at 70 °C for 180 min and then scanned between −500 and +500 mV for 100 cycles at 50 mV s^{-1} on an LK 98 microcomputer-based electrochemical analyzer (Tianjin, LANLIKE, China). The EIS measurement was carried out using a potentiostat/galvanostat (EG&G-PARC 273A) coupled to a lock-in amplifier (PARC model 5210) and a managing software. The impedance data were collected as a function of frequency scanned from the highest (10^5 Hz) to the lowest (0.001 Hz) using the "single-sine" (lock-in amplifier) method. The measurement was conducted in a conventional H-type electrochemical quartz cell with three compartments. During the measurement, a Pt plane was used as the counter electrode (area, 2×2 cm^2) and a saturated calomel electrode
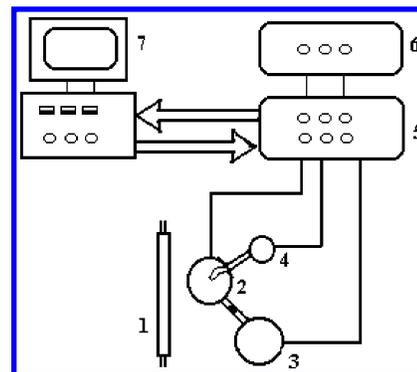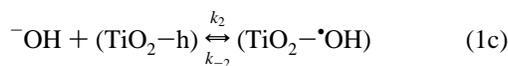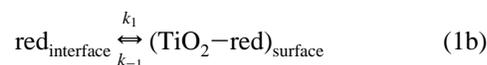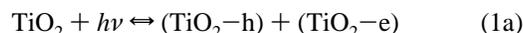

Figure 1. The setup of EIS measurement: 1 = UV lamp; 2 = working electrode; 3 = counter electrode; 4 = reference electrode; 5 = potentiostat/galvanostat; 6 = lock-in amplifier; 7 = computer.

(SCE) as the reference electrode. A bias was superimposed onto the photoelectrochemical system. A 365 nm light source (6 W) was used to illuminate the TiO_2/electrolyte interface. The experimental setup of EIS measurement was illustrated in Figure 1.

The initial pH in the solution was adjusted to 7.5 using 0.01 M $HClO_4$ and 0.01 M NaOH. The SSA was used as a model chemical in the EIS measurement system, and its initial concentration was 1.0×10^{-4} M after dark adsorption equilibrium.

3. EIS Mathematical Model for TiO$_2$ PEC Reaction

3.1. The Mechanism of TiO$_2$ PEC Oxidation. In this PEC reaction system, the oxidation reaction (substrate degradation) takes place on the anode, and the reduction reaction (removal of oxygen) occurs on the cathode. For the EIS measurement, we only need to consider the reactions taking place on the working electrode (anode). On the basis of the mechanism of photocatalytic reaction proposed by Hoffmann et al.,[2] the PEC process on the anode can be correspondingly expressed as follows:

$$TiO_2 + h\nu \Leftrightarrow (TiO_2-h) + (TiO_2-e) \qquad (1a)$$

$$red_{interface} \underset{k_{-1}}{\overset{k_1}{\Leftrightarrow}} (TiO_2-red)_{surface} \qquad (1b)$$

$$^-OH + (TiO_2-h) \underset{k_{-2}}{\overset{k_2}{\Leftrightarrow}} (TiO_2-{}^\bullet OH) \qquad (1c)$$

$$(TiO_2-{}^\bullet OH) + (TiO_2-red)_{surface} \underset{k_{-3}}{\overset{k_3}{\Leftrightarrow}} (TiO_2-ox)_{surface} + e \qquad (1d)$$

It is also possible that the hole can react directly with the organic substrate,[23] which belongs to the one-step charge-transfer process. Peter and co-workers have described such charge-transfer process in other photoelectrochemical systems, which were involved with an electrical bias in CdS[24] or p-InP[25] photoelectrodes. Under the pathway of direct oxidation by holes, steps 1c and 1d can be combined into step 1d′ as follows:

$$(TiO_2-h) + (TiO_2-red)_{surface} \underset{k'_{-3}}{\overset{k'_3}{\Leftrightarrow}} (TiO_2-ox)_{surface} + e \quad (1d')$$
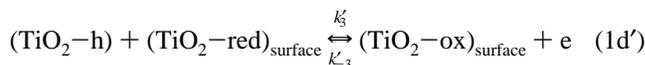
3.2. Setting Up of the EIS Model. Dark adsorption/desorption equilibrium of the substrate has already been established before any illumination in the PEC process. Once the illumination begins, the equilibrium will be rebalanced between the substrate degradation rate and further adsorption

rate.[26] During the PEC reaction, according to step 1b, a net adsorption rate in the EIS measurement can be expressed as follows:

$$\nu_1 = k_1(1 - \theta)C_A - k_{-1}\theta \tag{2}$$

According to the Hoffmann's mechanism (steps 1a, b, c, and d), steps 1a and 1c proceed fast and dynamic equilibrium can be quickly established, while there is no electron transfer in step 1b. Therefore, the Faradaic current density is mainly determined by step 1d.

Kuhne and Schefold[27] have proposed that under an electrical bias there is no potential barrier for the charge transfer between the energy levels of the semiconductor and the redox couple in the electrolyte; thus, the charge transfer is instantaneous. At the same time, the electrochemical reaction on the catalyst surface leads to polarization, as common for metal electrodes; therefore, the authors[27] have described the overvoltage for the hydrogen evolution on the illuminated photoelectrodes of blank and metal-coated p-type and n-type indium phosphide by the Butler−Volmer equation. Sato[28] has also described the rate of photoelectrode reactions on the basis of the theory of semiconductor electrode. In this reaction, while a hole is trapped to form a hydroxyl radical, an electron is simultaneously separated but just stored without contributing to the Faradaic current density as illustrated in steps 1a and 1c. Thereafter, once the hole trapped by the hydroxyl radical is released to oxidize the organic substrate, the substrate also releases another electron as indicated in step 1d. Thus the total Faradaic current density appears to be doubled. We extended the expression of Faradaic current density (I_F) on the n-type TiO$_2$ electrode according to Sato's theory,[28] as demonstrated in eq 3:

$$I_F = 2e[k_3 C_{\cdot OH}\theta - k_{-3}(1 - \theta)] \tag{3}$$

The rate constants of k_3 and k_{-3} depend on the electrode potential as shown in eqs 4 and 5:

$$k_3 = k_0 \exp\left(\frac{e\alpha}{kT}E\right) \tag{4}$$

$$k_{-3} = k_0 \exp\left[-\frac{e(1 - \alpha)}{kT}E\right] \tag{5}$$

Then eq 3 can be readily rewritten as follows:

$$I_F = 2ek_0\left\{C_{\cdot OH}\theta \exp\left(\frac{e\alpha}{kT}E\right) - (1 - \theta)\exp\left[-\frac{e(1 - \alpha)}{kT}E\right]\right\} \tag{6}$$

If the PEC reaction proceeds via the pathway of step 1d′, the Faradaic current density can be expressed as follows:

$$I'_F = 2ek_0\left\{\theta \exp\left(\frac{e\alpha}{kT}E\right) - (1 - \theta)\exp\left[-\frac{e(1 - \alpha)}{kT}E\right]\right\} \tag{6'}$$

The EIS model in this study is established on the basis of eq 6, which can be applied for all general cases. Up to now, we have obtained the expression of the I_F and need to determine the mathematical expression of the impedance of the PEC reaction based on the expression of admittance. In general, the I_F is related to the electrode potential (E), concentration of the surface states, concentration of the photogenerated carriers, e−h recombination, and θ. Under a steady state, other parameters can be assumed to be constant, except for E and θ, on the basis

of the analysis in the Introduction part; hence, I_F can be expressed as a function of E and θ. And during the PEC reaction, a deviation of I_F from the steady state is obtained by a small perturbation applied onto the working electrode (vs SCE). Such deviation can be expressed by the following equation in linear approximation using Taylor's series expansion:[29]

$$\Delta I_F = \left(\frac{\partial I_F}{\partial E}\right)_{ss}\Delta E + \left(\frac{\partial I_F}{\partial \theta}\right)_{ss}\Delta\theta \tag{7}$$

The ratio of $\Delta I_F/\Delta E$ is defined as Y_F. Then according to the method adopted by Leng et al.,[30] eq 8 can be obtained as follows:

$$Y_F = \frac{1}{R_t} + m\frac{\Delta\theta}{\Delta E} \tag{8}$$

Because during the impedance measurement the PEC degradation reaction of SSA proceeds very slowly at the steady state and the electrode state is not far from the equilibrium state, for the I_F at the steady state (I_0^E), I_+ is approximately equal to I_-, so eqs 9, 10, and 11 can be obtained:

$$I_F = I_+ - I_- \tag{9}$$

$$I_0^E = I_+ \cong I_- \tag{10}$$

Thus compared to eq 6, I_0^E can be expressed as

$$I_0^E = 2ek_0 C_{-OH}\theta \exp\left(\frac{e\alpha}{kT}E\right) =$$
$$2ek_0(1 - \theta)\exp\left[-\frac{e(1 - \alpha)}{kT}E\right] \tag{11}$$

Readily combined with eq 11, m and $1/R_t$ can be expressed as eqs 12 and 13, respectively, from eq 6 under the condition of steady state:

$$m = \left(\frac{\partial I_F}{\partial \theta}\right)_{ss} = \frac{I_0^E}{\theta} - \left(-\frac{I_0^E}{1 - \theta}\right) = \frac{I_0^E}{\theta(1 - \theta)} \tag{12}$$

$$\frac{1}{R_t} = \left(\frac{\partial I_F}{\partial E}\right)_{ss} = \frac{e\alpha}{kT}I_0^E + \frac{e(1 - \alpha)}{kT}I_0^E = \frac{e}{kT}I_0^E \tag{13}$$

Now, $\Delta\theta/\Delta E$ in eq 8 needs to be obtained. According to eqs 1d and 2, the $\dot\theta$ can be described as

$$\Gamma_{max}\dot\theta = \Gamma_{max}\frac{d\theta}{dt} = -\frac{I_F}{F} + k_1(1 - \theta)C_A - k_{-1}\theta \tag{14}$$

Note that in eq 14, the item of $-I_F/F$ corresponds to step 1d (electrochemical reaction rate relating to θ) and the item of $k_1(1 - \theta)C_A - k_{-1}\theta$ corresponds to step 1b (the net adsorption rate relating to θ).

Under the perturbation of small amplitude, the derivation of $\dot\theta$ from the steady state can be expressed by the following equation in a linear approximation using Taylor's serials expansion:

$$\Gamma_{max}\Delta\dot\theta = \Gamma_{max}\frac{d\Delta\theta}{dt} = \left(\frac{\partial\dot\theta}{\partial I}\right)_{ss}\Delta I + \left(\frac{\partial\dot\theta}{\partial\theta}\right)_{ss}\Delta\theta = -\frac{1}{F}\Delta I +$$
$$\left[-\frac{\partial(k_1 C_A + k_{-1})\theta}{\partial\theta}\right]_{ss}\Delta\theta = -\Delta I/F - (k_1 C_A + k_{-1})\Delta\theta \tag{15}$$
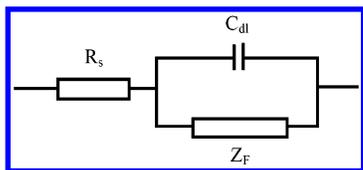
Figure 2. The impedance of the electrode system defined by Cao and Zhang.[31]

At the same time, the response of $\Delta\theta$ to the small sinusoidal perturbation with an angular frequency ω should be represented as an ac sinusoidal signal with the same ω; consequently,

$$\Delta\dot{\theta} = j\omega\Delta\theta \tag{16}$$

Also,

$$\Delta I_F = \left(\frac{\partial I_F}{\partial E}\right)_{ss}\Delta E + \left(\frac{\partial I_F}{\partial\theta}\right)_{ss}\Delta\theta$$

$$= \left(\frac{1}{R_t}\right)\Delta E + m\Delta\theta \tag{17}$$

Combination of eqs 15, 16, and 17 yields eq 18,

$$\frac{\Delta\theta}{\Delta E} = -\frac{\dfrac{1}{R_t}}{F\Gamma_{max}j\omega + m + F(k_1C_A + k_{-1})} \tag{18}$$

Substitution of eq 18 for eq 8 leads to

$$Y_F = \frac{1/R_t}{1 + \dfrac{m}{F\Gamma_{max}j\omega + F(k_1C_A + k_{-1})}} \tag{19}$$

Cao and Zhang[31] defined the relationship between Y_F and Z_{EIS} as illustrated in Figure 2, so the impedance of the photoelectrochemical system can be expressed as follows when the Y_F is known ($Y_F = 1/Z_F$):

$$Z_{EIS} = R_s + \frac{1}{j\omega C_{dl} + Y_F} \tag{20}$$

Combination of eqs 19, 20, and 12 and then rearrangement leads to the EIS expression of the PEC reaction system:

$$Z_{EIS} = R_s + \frac{1}{j\omega C_{dl} + \dfrac{1}{R_t + \dfrac{\dfrac{I_0^E}{\theta(1-\theta)}R_t}{F\Gamma_{max}j\omega + F(k_1C_A + k_{-1})}}} \tag{21}$$

4. Results and Discussion

4.1. Theoretical Simulation Using the EIS Model. In this study, the Faradaic current density at steady state (I_0^E) in the EIS measurement was presumed to be in the range of 10^{-6}–10^{-4} A cm^{-2}. The capacitance of double layer (C_{dl}) generally from several tens to hundreds of microfarads per square centimeter is assumed here to be 8.0×10^{-4} F cm^{-2}, while the charge-transfer resistance (R_t) can be calculated from the given value of I_0^E by eq 13. The saturation adsorption amount of SSA onto the H-TiO$_2$ was determined to be 2.0×10^{-6} mol g^{-1} on the basis of the previous adsorption isotherm experimental results[32] as illustrated in Figure 3. And the active area of the
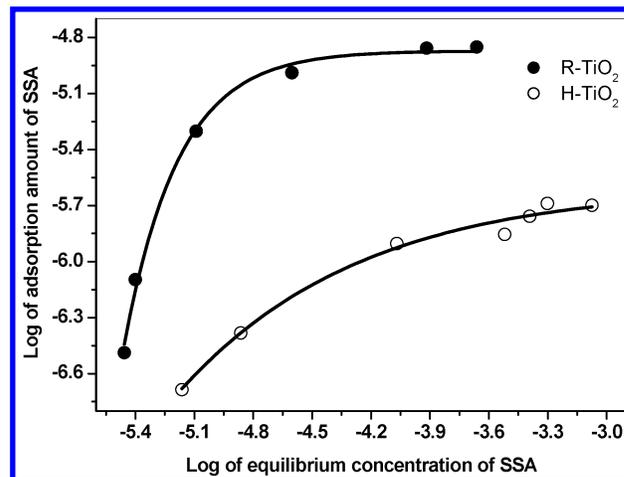

Figure 3. The SSA adsorption isotherms on H-TiO$_2$ and R-TiO$_2$.

coated H-TiO$_2$ was determined to be 200 cm^2 g^{-1} because around 5 mg of TiO$_2$ powder was supported on 1×1 cm^2 flat electrode as given in the Experimental Section. Accordingly, the maximum adsorption amount of organic substrate on the TiO$_2$ electrode (Γ_{max}) can be calculated approximately to be 1.0×10^{-8} mol cm^{-2}. The adsorption equilibrium constant of SSA on the TiO$_2$ ($k_a = k_1/k_{-1}$) can be determined by applying the Langmuir adsorption model (eq 23) to fit the data obtained also in the adsorption isotherm experiment as illustrated in Figure 3. The values of k_1 and k_{-1} need to be assumed with a fixed ratio of $k_a = k_1/k_{-1}$. The fraction of surface coverage of adsorbed organic on TiO$_2$ surface (θ) according to eq 2 can be expressed as follows:

$$\theta = \frac{k_1C_A}{k_1C_A + k_{-1}} \tag{22}$$

Obviously, eq 22 can be rewritten as the Langmuir adsorption model:

$$\theta = \frac{k_aC_A}{1 + k_aC_A} \tag{23}$$

Then the value of θ can be calculated from eq 23.

Under the above conditions, the theoretical simulation results of eq 21 are illustrated in Figure 4, in which the values of H-TiO$_2$ parameters are used as an example. It can be seen from Figure 4 that when the I_0^E is high enough (1.0×10^{-4} A cm^{-2}), two arcs/semicircles (curve 1) occur on the EIS plane display of the PEC reaction; when the I_0^E decreases from 1.0×10^{-4} to 1.1×10^{-5} A cm^{-2}, the two arcs/semicircles evolve to one arc/semicircle (curve 4). In the meantime, it can also be noted that when the I_0^E decreases from 1.0×10^{-4} to 1.1×10^{-5} A cm^{-2}, the diameter of the first arc (under the higher frequency) increases correspondingly, but the diameter of the second arc (under the lower frequency) has no change. It indicates that the first arc is affected by the I_0^E and represents the charge-transfer step. Finally, it can be concluded that the big single semicircle as curve 4 results from the enlargement of the first arc, when the I_0^E is very small.

On the other hand, the EIS plane display can also be affected by θ, as illustrated in Figure 5. When the θ value decreases from 0.35 to 0.17 (curves 1−3), the diameter of the second arc increases, but the diameter of the first arc stays constant. These results contrast with the results in Figure 4. Because θ is the factor affecting the adsorption rate, this indicates that the second
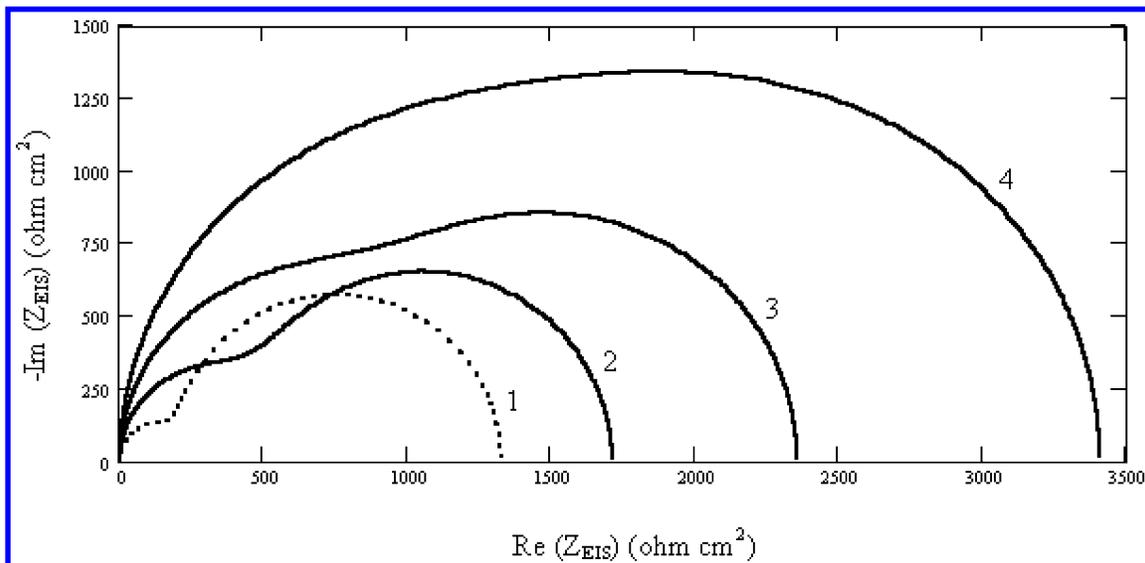
Figure 4. Simulated EIS plane display of PEC reaction under $\theta = 0.17$, $T = 298$ K, $C_{dl} = 8.0 \times 10^{-4}$ F cm^{-2}, $k_1 = 3 \times 10^{-6}$ cm, $k_{-1} = 1.5 \times 10^{-9}$ mol cm^{-2}, $\Gamma_{max} = 1.0 \times 10^{-8}$ mol cm^{-2}, $C_A = 1.0 \times 10^{-4}$ M, $R_{ads} = 1065$ Ω cm^2, $R_s = 5$ Ω cm^2, and different I_0^E: (curve 1) 1.0×10^{-4}; (curve 2) 4.0×10^{-5}; (curve 3) 2.0×10^{-5}; (curve 4) 1.1×10^{-5} A cm^{-2}. The calculation of R_{ads} can be found in the Appendix.
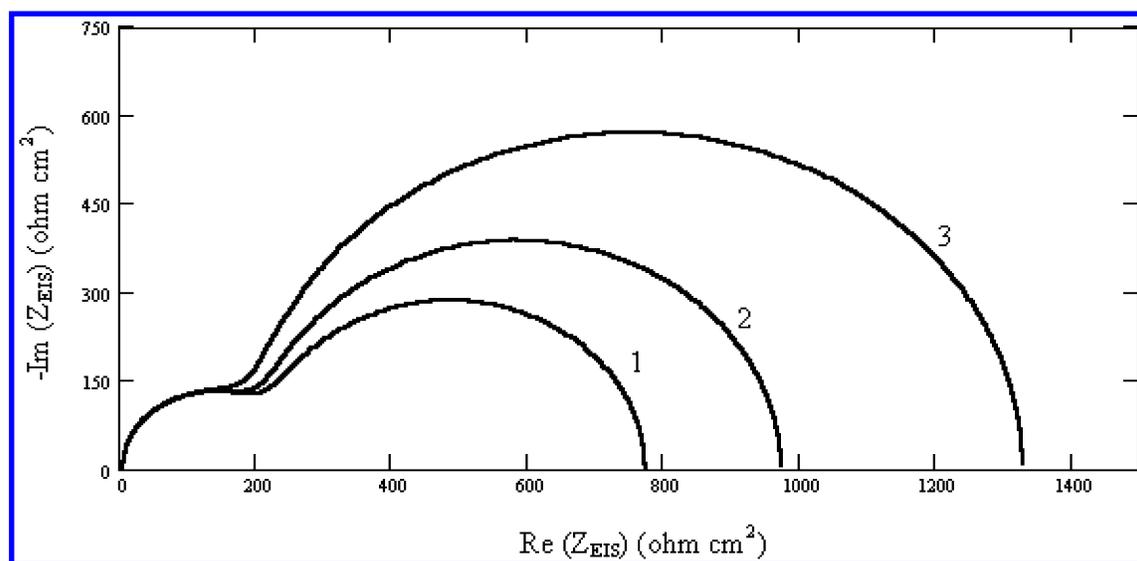

Figure 5. Simulated EIS plane display of PEC reaction under $I_0^E = 1.0 \times 10^{-4}$ A cm^{-2}, $T = 298$ K, $C_{dl} = 8.0 \times 10^{-4}$ F cm^{-2}, $k_{-1} = 1.5 \times 10^{-9}$ mol cm^{-2}, $\Gamma_{max} = 1.0 \times 10^{-8}$ mol cm^{-2}, $C_A = 1.0 \times 10^{-4}$ M, $R_t = 257.0$ Ω cm^2, $R_s = 5$ Ω cm^2, and different θ and k_1: (curve 1) $\theta = 0.35$, $k_1 = 8.0 \times 10^{-6}$ cm; (curve 2) $\theta = 0.25$, $k_1 = 5.0 \times 10^{-6}$ cm; (curve 3) $\theta = 0.17$, $k_1 = 3.0 \times 10^{-6}$ cm.

arc represents the adsorption step. Moreover, under this condition of $I_0^E = 1.0 \times 10^{-4}$ A cm^{-2}, even if the θ value further decreases to a very small value of 0.032 and the second arc becomes very large (not shown here), there are still two arcs on the EIS plane display. These results can further confirm that the single semicircle as curve 4 in Figure 4 is affected dominantly by the charge-transfer step but not the adsorption step. Under the condition of a larger $I_0^E = 5.0 \times 10^{-4}$ A cm^{-2} and other conditions being the same as those in Figure 5, when the θ value decreases to 0.032 and the adsorption arc becomes very large, the first arc (charge-transfer arc) can be covered as illustrated in Figure 6.

4.2. Experimental EIS Plane Display of the SSA PEC Reactions. To investigate the agreement between the indication by the model of eq 21 and the experimental results, the EIS measurements were performed in the SSA PEC reaction using the H-TiO$_2$ as a catalyst. The experimental results are illustrated in Figure 7. It can be seen that the experiment demonstrated a similar phenomenon to the theoretical simulation results. When

the externally applied bias was below 200 mV (vs SCE), there was only one arc/semicircle on the EIS plane display. When the bias exceeded 200 mV (vs SCE), two arcs turned up. Furthermore, the diameter of the first arc (under the high frequency) increased with the bias decrease, but the second arc was not affected. Now it can be concluded that of the two arcs on the EIS plane display, the first one represents the charger-transfer step and the second one (under a low frequency) represents the adsorption step.

To further confirm the indication from the theoretical simulation results with a low value of I_0^E, the second set of SSA PEC reaction experiments was conducted using two different TiO$_2$ samples of H-TiO$_2$ and R-TiO$_2$, in which a low electrical bias of 150 mV was applied and EIS was measured during the PEC reaction. The results of EIS shown in Figure 8 demonstrated that only one arc/semicircle was observed under this reaction condition. These results are in good agreement with the theoretical indication as shown in Figure 4. However, this single arc/semicircle could be either the first arc representing
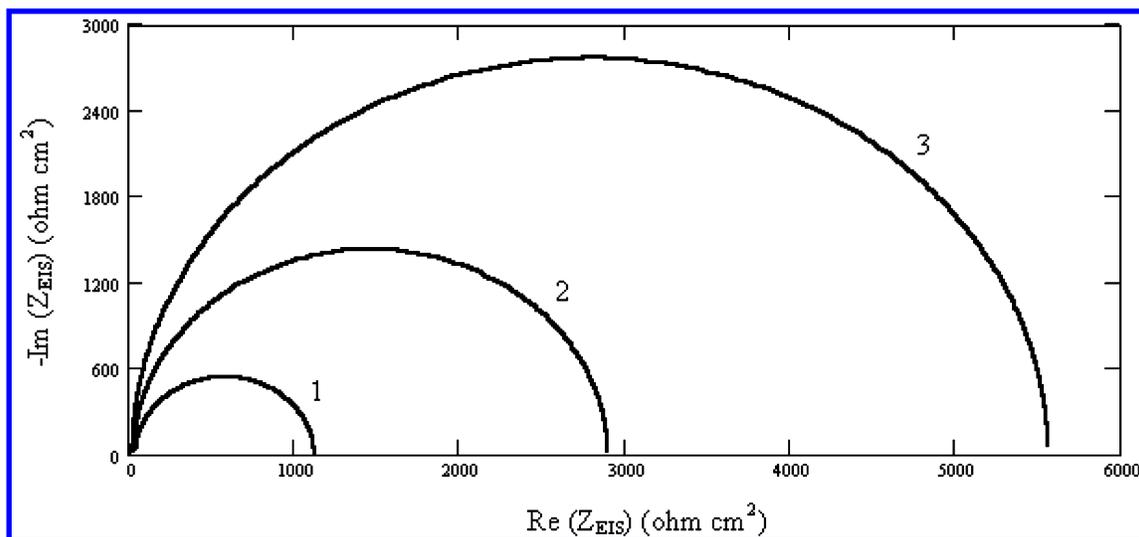
An Alternative Approach to Ascertain

J. Phys. Chem. B, Vol. 107, No. 34, 2003 **8993**

Figure 6. Simulated EIS plane display of PEC reaction under $I_0^E = 5.0 \times 10^{-4}$ A cm^{-2}, $T = 298$ K, $R_t = 51.4$ Ω cm^2, $C_{dl} = 8.0 \times 10^{-4}$ F cm^{-2}, $k_{-1} = 1.5 \times 10^{-9}$ mol cm^{-2}, $\Gamma_{max} = 1.0 \times 10^{-8}$ mol cm^{-2}, $C_A = 1.0 \times 10^{-4}$ M, $R_s = 5$ Ω cm^2, and different θ and k_1: (curve 1) $\theta = 0.17$, $k_1 = 3.0 \times 10^{-6}$ cm; (curve 2) $\theta = 0.062$, $k_1 = 1.0 \times 10^{-6}$ cm; (curve 3) $\theta = 0.032$, $k_1 = 5.0 \times 10^{-7}$ cm.
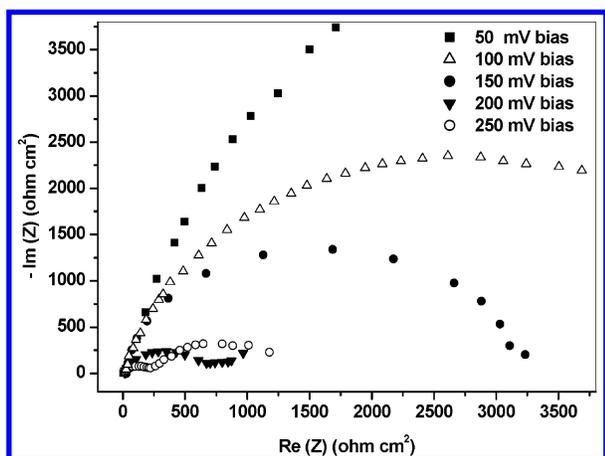

Figure 7. Effect of external bias on the EIS plane display of the PEC reaction using the H-TiO$_2$ photoelectrode.
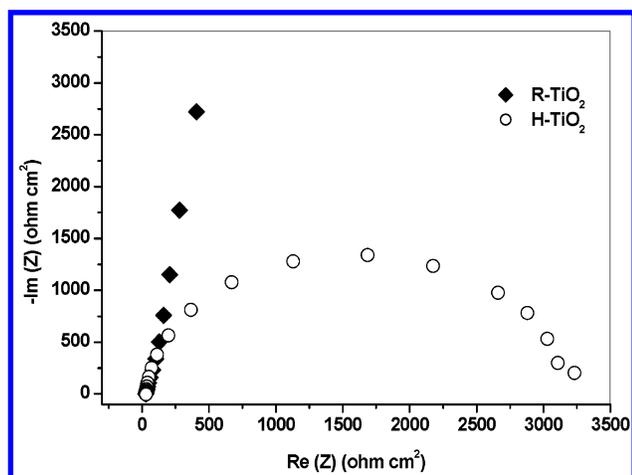

Figure 8. The EIS plane display in the experiments using different TiO$_2$ electrodes with the applied external bias of 150 mV (vs SCE).

the surface charge-transfer step or the second arc representing the adsorption step, because one arc might be covered by the other as indicated by curve 4 in Figure 4 and curve 3 in Figure 6. If this single arc/semicircle represents the adsorption step in the PEC reaction, its diameter should increase as the adsorption ability of catalyst becomes weaker. On the basis of the results

in the adsorption isotherm experiment as shown in Figure 3, the adsorption ability of H-TiO$_2$ is weaker than that of R-TiO$_2$ significantly; therefore, the arc/semicircle of H-TiO$_2$ should be larger than that of R-TiO$_2$ if the arc/semicircle represents the adsorption step. However, the results shown in Figure 8 revealed an opposite situation, that the EIS arc/semicircle of H-TiO$_2$ was significantly smaller than that of R-TiO$_2$. This result confirms that the RDS in this reaction must not be the adsorption step represented by the second arc/semicircle as shown by curve 4 in Figure 4. On the other hand, it has been established in our previous studies that the H-TiO$_2$ had better photoactivity than the R-TiO$_2$ due to a thermal hydrogen treatment.[22] Comparing the EIS results of H-TiO$_2$ and R-TiO$_2$ in Figure 8, the diameter of H-TiO$_2$ arc is smaller than that of R-TiO$_2$ significantly. These results confirm that the single arc/semicircle shown in Figure 8 must be the first arc/semicircle representing the surface charge-transfer step in the PEC reaction.

4.3. The RDS of the Photoelectrocatalytic Reaction. From the EIS simulation results of the PEC reaction as shown in Figure 4, it has been indicated that if two arcs/semicircles are observed in the EIS display, it implies the existence of two RDS (both the charge-transfer step and adsorption step) in the reaction and if only one arc/semicircle is observed, it indicates the existence of only one RDS in the reaction. This theoretical indication has been confirmed by the experimental results as shown in Figures 7 and 8. It is believed that either the surface charge-transfer step or adsorption step or both steps can be the RDS in the TiO$_2$ PEC reaction under certain conditions. The results of EIS measurement indicate that when the externally applied bias was lower than 200 mV (vs SCE), there was only one arc/semicircle on the EIS plane display, suggesting that only the surface charge-transfer step is the RDS in the reaction. When the externally applied bias exceeded 200 mV (vs SCE), there were two arcs/semicircles on the EIS plane display, indicating that both the surface charge-transfer step and adsorption step are the RDS in the reaction. Furthermore, it can be inferred from Figure 4 that when the charge-transfer step proceeds slowly, the adsorption step is a fast step relatively, so it can be neglected and only the charge-transfer step is the RDS. Only when the charge-transfer step proceeds rapidly enough, the adsorption step can become important and then become another RDS.
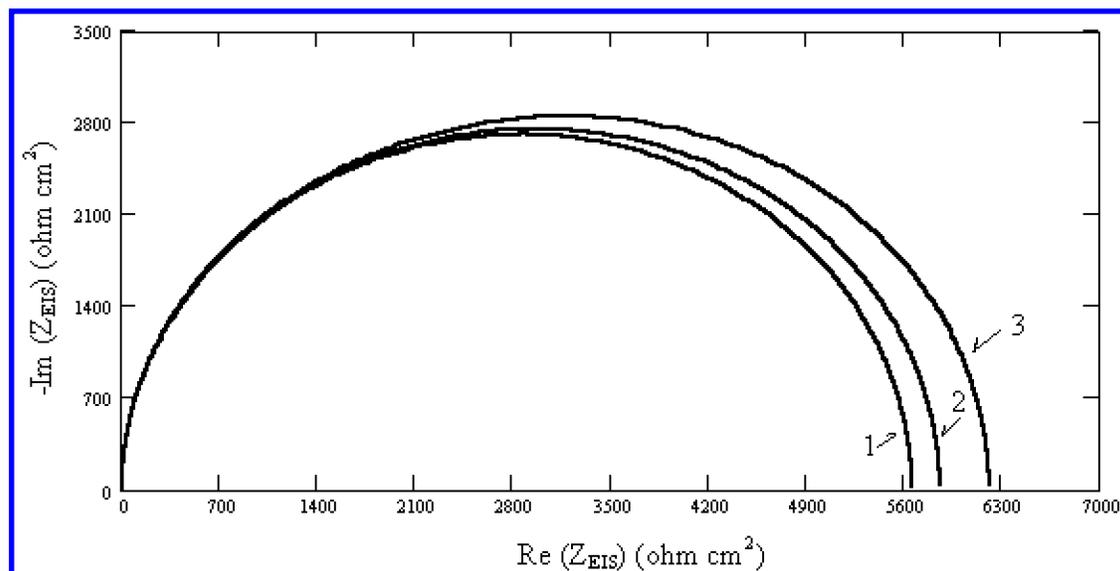
Figure 9. Theoretical effect of adsorption on the EIS plane display under $I_0^E = 5.0 \times 10^{-6}$ A cm^{-2}, $T = 298$ K, $R_t = 5140$ Ω cm^2, $C_{dl} = 8.0 \times 10^{-4}$ F cm^{-2}, $k_{-1} = 1.5 \times 10^{-9}$ mol cm^{-2}, $\Gamma_{max} = 1.0 \times 10^{-8}$ mol cm^{-2}, $C_A = 1.0 \times 10^{-4}$ M, $R_s = 5$ Ω cm^2, and different θ and k_1: (curve 1) $\theta = 0.35$, $k_1 = 8.0 \times 10^{-6}$ cm; (curve 2) $\theta = 0.25$, $k_1 = 5.0 \times 10^{-6}$ cm; (curve 3) $\theta = 0.17$, $k_1 = 3 \times 10^{-6}$ cm.
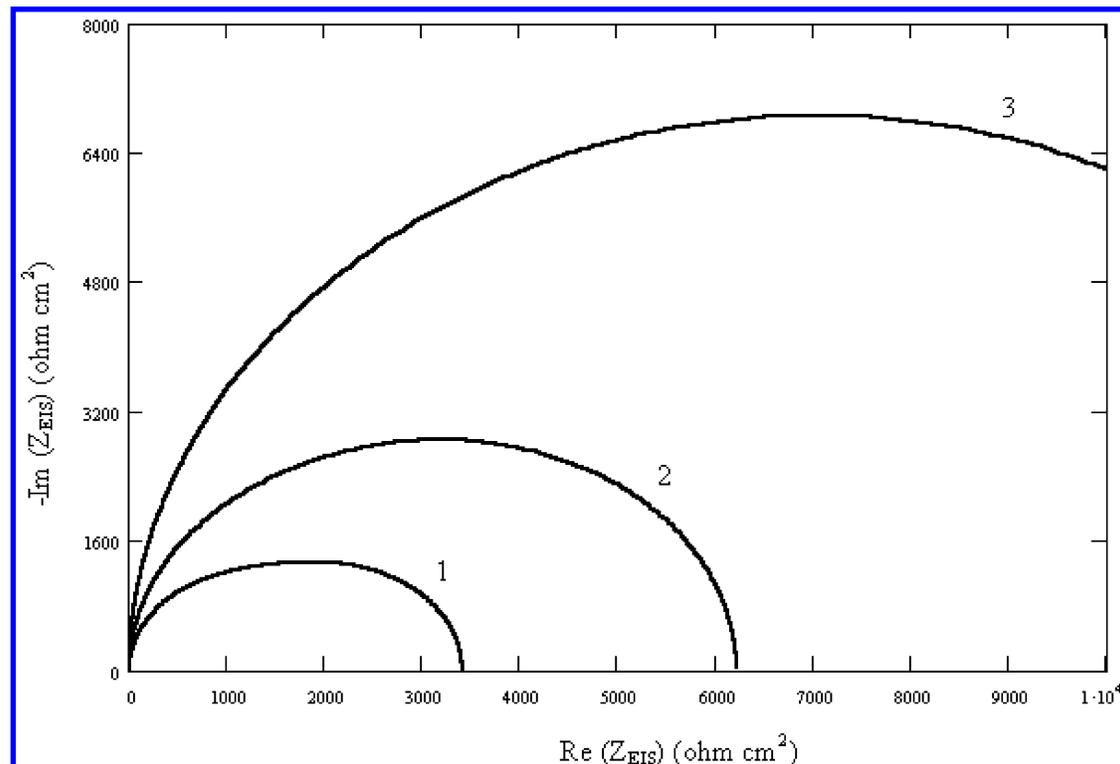

Figure 10. Simulated EIS plane display of the PEC reaction under $\theta = 0.17$, $T = 298$ K, $R_{ads} = 1065$ Ω cm^2, $C_{dl} = 8.0 \times 10^{-4}$ F cm^{-2}, $k_1 = 3.0 \times 10^{-6}$ cm, $k_{-1} = 1.5 \times 10^{-9}$ mol cm^{-2}, $\Gamma_{max} = 1.0 \times 10^{-8}$ mol cm^{-2}, $C_A = 1.0 \times 10^{-4}$ M, $R_s = 5$ Ω cm^2, and different low I_0^E values: (curve 1) 1.1×10^{-5}; (curve 2) 5.0×10^{-6}; (curve 3) 2.0×10^{-6} A cm^{-2}.

4.4. The Effects of Adsorption and Charge-Transfer Rate on the EIS. According to eq 21, several variables (θ, k_1, k_{-1}, Γ_{max}) are related to the adsorption. Here, we change the value of k_1 to obtain different θ values through eq 23 to conduct the EIS simulation using eq 21. When a low I_0^E is given and the θ value reduces from 0.35 to 0.17, the results are illustrated in Figure 9. It can be seen that there is only one arc/semicircle on the EIS plane display due to a low value of I_0^E and the diameter of the single arc/semicircle increases insignificantly when θ reduces. At the same time, when there is only one arc/semicircle

on the EIS plane display under low I_0^E, the effect of I_0^E on the arc/semicircle diameter is significant as illustrated in Figure 10.

On the other hand, when there are two arcs/semicircles on the EIS plane display under a high I_0^E value as illustrated in Figure 5, the same change of θ value from 0.35 to 0.17 affects the diameter of the second arc/semicircle much more significantly. Consequently, it can be concluded that under low I_0^E, the RDS in the reaction is dominated by the charge-transfer step but not the adsorption step very remarkably and that under high I_0^E, when the charge transfer rate becomes fast enough,

An Alternative Approach to Ascertain

J. Phys. Chem. B, Vol. 107, No. 34, 2003 **8995**

both the rates of charge-transfer step and adsorption step should be considered to affect the EIS plane display obviously as RDS in the PEC reaction.

From the above results, it can be further discussed that in the PEC reaction using SSA as the organic substrate, when the surface charge-transfer step is slow, it acts as the RDS. When it proceeds rapidly, adsorption can become another RDS. This suggests that if the surface charge-transfer step proceeds slowly, the measures adopted to increase the reaction rate by increasing the organic adsorption appears not effective because it is not an RDS. On the other hand, if the surface charge-transfer step proceeds rapidly and two RDS of both the adsorption and the surface charge-transfer steps are predominant, the reaction rate can be accelerated by improving the organic adsorption behavior as well. Of course, under either case, any measures to enhance the surface charge-transfer step will be effective to speed up the PEC reaction rate.

4.5 Application of the EIS Method in a PEC Oxidation Process. The EIS method studied in this work has a purpose to simulate an equivalent PEC reaction process. It has been agreed that either the charge transfer or the adsorption on the photoelectrodes are the main potential steps to control a PEC oxidation reaction. In the EIS model, changing the parameters of I_0^E and the fraction of surface coverage θ represents the variation of the charge-transfer rate and adsorption rate in the PEC reaction, respectively. This mathematical model has indicated three typical reactions with different RDS in the PEC process as shown in Figures 4−6. (1) If the I_0^E is very low, there is only one arc/semicircle on the EIS display. It indicates the charge-transfer rate is much slower than the adsorption rate and the charge-transfer step is the only RDS in the reaction. (2) If the I_0^E becomes higher, there are two arcs/semicircles on the EIS display. It indicates that the charge-transfer rate increases and becomes equivalent to the adsorption rate. Both the steps become the RDS in the reaction. (3) If the I_0^E is further increased and the adsorption step becomes slow enough relatively, there is only one arc/semicircle again. It indicates that the charge-transfer rate is much faster than the adsorption rate and the adsorption step becomes the RDS in the reaction. The first two reactions have been confirmed in the EIS measurement experiments by either applying different electrical biases or using the catalysts with different adsorption abilities as shown in Figures 7 and 8, respectively. The third reaction has not been observed in this work because the PEC heterogeneous reaction will not proceed rapidly enough, if the θ value is quite low representing a slow adsorption rate in practice. The application of the EIS measurement is an easier way to determine the RDS in a PEC oxidation process. If the RDS in the EIS experiment is found to be the charge-transfer step, the consideration of how to improve the PEC oxidation should be focused on the increase of PEC reaction rate by increasing the external bias, light intensity, catalyst activity, or pH conditions. If the RDS is the adsorption step, improving the adsorption conditions in the process should be addressed.

5. Summary

An EIS mathematical model has been established on the basis of the TiO$_2$ PEC mechanism. The model indicates three typical reactions in a PEC oxidation process, which include the charge-transfer-dominated reaction, both the charge-transfer- and adsorption-dominated reaction, and the adsorption-dominated reaction. The EIS model indication has been confirmed by conducting the EIS measurement in a set of the PEC oxidation of SSA solutions in a TiO$_2$-coated photoelectrode reactor system.

The experimental results showed that there were two capacitive arcs/semicircles under a high electrical bias applied, corresponding to both the charge-transfer- and adsorption-dominated reaction, and that there was only one capacitive arc/semicircle under a low bias, corresponding to the charge-transfer-dominated reaction. But, the adsorption-dominated reaction was not observed in this work. The experimental results have a good agreement with the model simulation. The EIS method in this study provides an easier way to determine the RDS in a PEC oxidation process, which would be helpful to better control the reaction in practice.

Appendix

Equation 21 can be rewritten as the following form:

$$Z_{\text{EIS}} = R_s + \cfrac{1}{j\omega C_{\text{dl}} + \cfrac{1}{R_t + \cfrac{1}{j\omega C_{\text{ads}} + \cfrac{1}{R_{\text{ads}}}}}} \qquad \text{(A1)}$$

A comparison of eq A1 and eq 21 yields

$$R_{\text{ads}} = \frac{mR_t}{F(k_1 C_A + k_{-1})} \qquad \text{(A2)}$$

Substitution of m and R_t by eqs 12 and 13, respectively, and rearrangement lead to

$$R_{\text{ads}} = \frac{kT}{eFk_{-1}\theta} \qquad \text{(A3)}$$

Also substitution of θ in eq A3 by eq 23 and rearrangement yield

$$R_{\text{ads}} = \frac{kT}{eFk_{-1} \cfrac{C_A}{C_A + \cfrac{1}{k_a}}} \qquad \text{(A4)}$$

Nomenclature

C_A = organic substrate concentration near the surface of TiO$_2$
C_{ads} = capacitance of adsorption, F cm^{-2}
C_{dl} = capacitance of double layer, F cm^{-2}
$C_{\bullet\text{OH}}$ = $^{\bullet}$OH radical concentration
E = electrode potential, V
e = electron or photogenerated electron(s), -1.602×10^{-19} C
F = Faradaic constant, 9.65×10^4 C mol^{-1}
h = photogenerated hole(s)
I_+, I_- = Faradaic current density, A cm^{-2}, for oxidation reaction and reduction reaction, respectively
I_0^E = Faradaic current density at steady state, A cm^{-2}
I_F, I_F' = Faradaic current density, A cm^{-2}
$j = \sqrt{-1}$

k = Boltzmann constant, 1.38×10^{-23} J K^{-1}

k_a = adsorption equilibrium constant

k_i, $i = \pm1, \pm2, \pm3$ = reaction rate constants, + means forward reaction and − means backward reaction

$m = (\partial I_F / \partial \theta)_{ss}$, A cm^{-2}

R_{ads} = adsorption resistance, Ω cm^2

R_s = solution resistance, Ω cm^2

$1/R_t = (\partial I_F / \partial E)_{ss}$, charge-transfer resistance, Ω cm^2

ss = subscript denoting steady state

T = absolute temperature

t = time, s

θ = fraction of surface coverage of adsorbed organic substrate on TiO$_2$ surface

$\dot{\theta}$ = changing rate of θ with time

Y_F = Faradaic admittance of photoelectrochemical system, Ω^{-1} cm^{-2}

Z_{EIS} = impedance of photoelectrochemical system, Ω cm^2

α = transfer coefficient

ω = angular frequency, s^{-1}

Γ_{max} = maximum adsorption amount of organic substrate on the TiO$_2$ electrode, mol cm^{-2}

ν_1 = net adsorption reaction rate, that is, dθ/dt

References and Notes

(1) Ollis, D. F. *Environ. Sci. Technol.* **1985**, *19*, 480.

(2) Hoffmann, M. R.; Martin, S. T.;. Choi, W.; Bahnemann, D. W. *Chem. Rev.* **1995**, *95*, 69.

(3) Bianco, A.; Vincenti, M.; Bianciotto, A.; Pramauro, E. *Appl. Catal. B: Environ.* **1999**, *22*, 149.

(4) Vinodgopal, V.; Hotchandani, S.; Kamat, P. V. *J. Phys. Chem.* **1993**, *97*, 9040.

(5) Kim, H.; Anderson, C. *Environ. Sci. Technol.* **1994**, *28*, 479.

(6) Vinodgopal, V.; Kamat, P. V. *Environ. Sci. Technol.* **1995**, *29*, 841.

(7) Kesselman, J. M.; Lewis, N. S.; Hoffmann, M. R. *Environ. Sci. Technol.* **1997**, *31*, 2298.

(8) Calvo, M. E.; Candal, R. J.; Bilmes, S. A. *Environ. Sci. Technol.* **2001**, *35*, 4132.

(9) Mandelbaum, P.; Bilmes, S. A.; Begazzoni, A. E.; Blesa, M. A. *Sol. Energy* **1999**, *65*, 75.

(10) Li, X. Z.; Liu, H. L.; Yue, P. T.; Sun, Y. P. *Environ. Sci. Technol.* **2000**, *34*, 4401.

(11) Fernandez-Ibanez, P.; Malato, S.; Enea, O. *Catal. Today* **1999**, *54*, 329.

(12) Zhang, F.; Zhao, J.; Shen, T.; Hidaka, H.; Pelizzetti, E.; Serpone, N. *Appl. Catal., B* **1998**, *15*, 147.

(13) Sauer, T.; Neto, G. C.; José, H. J.; Moreira, R. F. P. M. *J. Photochem. Photobiol., A* **2002**, *149*, 147.

(14) Yamazaki, S.; Tanaka, S.; Tsukam, H. *J. Photochem. Photobiol., A* **1999**, *121*, 55.

(15) Kim, Y.; Ikebukuro, K.; Muguruma, H.; Karube, I. *J. Biotechnol.* **1998**, *59*, 213.

(16) Conway, B. E.; Bockris, J. O'M.; White, R. E. *Modern Aspects of Electrochemistry*; Kluwer Academic/Plenum Publishers: New York, 1999; No. 32, p 143.

(17) Marsh, J.; Gorse, D. *Electrochim. Acta* **1998**, *43*, 659.

(18) Bisquert, J.; Garcia-Belmonte, G.; Fabregat-Santiago, F.; Ferriols, N. S.; Bogdanoff, P.; Pereira, E. C. *J. Phys. Chem. B* **2000**, *104*, 2287.

(19) Meier, A.; Selmarton, D. D.; Siemoneit, K.; Smith, B. B.; Nozik, A. J. *J. Phys. Chem. B* **1999**, *103*, 2122.

(20) Liu, H.; Cheng, S. A.; Wu, M.; Wu, H. J.; Zhang, J. Q.; Li, W. Z.; Cao, C. N. *J. Phys. Chem. A* **2000**, *104*, 7016.

(21) Leng, W. H.; Zhang, Z.; Cheng, S. A.; Zhang, J. Q.; Cao, C. N. *Chin. Chem. Lett.* **2001**, *12*, 1019.

(22) Liu, H.; Ma, H. T.; Li, X. Z.; Li, W. Z.; Wu, M.; Bao, X. H. *Chemosphere* **2003**, *50*, 39.

(23) Rajeshwar, K. *J. Appl. Chem.* **1995**, *25*, 1067.

(24) Fermin, D. J.; Ponomarev, E. A.; Peter, L. M. *J. Electroanal. Chem.* **1999**, *473*, 192.

(25) Ponomarev, E. A.; Peter L. M. *J. Electroanal. Chem.* **1995**, *397*, 45.

(26) Xu, Y. M.; Langford, C. H. *Langmuir* **2001**, *17*, 897.

(27) Kuhne, H.-M.; Schefold, J. *J. Electrochem. Soc.* **1990**, *137*, 568.

(28) Sato, N. *Electrochemistry at metal and semiconductor electrodes*; Elsevier: Amsterdam, 1998; p 352.

(29) Cao, C. N. *Electrochim. Acta* **1990**, *35*, 831.

(30) Leng, Y. J.; Zhang, J. Q.; Cheng, S. A.; Cao, C. N.; Ye, Z. S. *Electrochim. Acta* **1998**, *43*, 1945.

(31) Cao, C. N.; Zhang J. Q. *An Introduction to Electrochemical Impedance Spectroscopy*; Science Press: Beijing, China, 2002; p 37.

(32) Liu, H.; Cheng, S. A.; Zhang, J. Q.; Cao, C. N.; Zhang, S. K. *Chemosphere* **1999**, *38*, 283.